PHILOSOPHICAL TRANSACTIONS OF THE ROYAL SOCIETY A MATHEMATICAL, PHYSICAL & ENGINEERING SCIENCES

Density and Composition of the Lower Mantle

R. Jeanloz and Elise Knittle

Phil. Trans. R. Soc. Lond. A 1989 **328**, 377-389
doi: 10.1098/rsta.1989.0042

Phil. Trans. R. Soc. Lond. A **328**, 377–389 (1989)
Printed in Great Britain

Density and composition of the lower mantle

By R. Jeanloz and Elise Knittle

Department of Geology and Geophysics, University of California, Berkeley, California 94720, *U.S.A.*

The observed density distribution of the lower mantle is compared with density measurements of the (Mg,Fe)SiO_3 perovskite and (Mg,Fe)O magnesiowüstite high-pressure phases as functions of pressure, temperature and composition. We find that for plausible bounds on the composition of the upper mantle (ratio of magnesium to iron + magnesium components $x_{Mg} \geqslant 0.88$) and the temperature in the lower mantle ($T \geqslant 2000$ K), the high-pressure mineral assemblage of upper-mantle composition is at least 2.6 (± 1) % less dense than the lower mantle over the depth range 1000–2000 km. Thus, we find that a model of uniform mantle composition is incompatible with the existing mineralogical and geophysical data. Instead, we expect that the mantle is stratified, with the upper and lower mantle convecting separately, and we estimate that the compositional density difference between these regions is about 5 (± 2) %. The stratification may not be perfect ('leaky layering'), but significant intermixing and homogenization of the upper and lower mantle over geological timescales are precluded.

Introduction

The purpose of this study is to interpret the density distribution through the Earth's lower mantle in terms of the bulk composition of this region. Specifically, we examine the degree to which an upper-mantle composition can satisfy the observed properties of the lower mantle. The reason for doing this is that whereas the uppermost mantle can be directly sampled and examined through the analysis of xenoliths and other rock fragments that are brought volcanically or tectonically to the surface, it is the lower mantle that makes up the bulk of our planet: almost 50 % by mass and over 61 % on an atomic basis. The problem, therefore, is to decide whether or not the outermost regions of the Earth that can be sampled are representative of the silicate portion of our planet, most of which cannot be directly observed.

We emphasize the analysis of density, rather than elastic moduli or wave velocities, because this is a relatively well-known property both for the Earth's interior and for candidate mineral assemblages existing at the pressures and temperatures of the deep mantle. The density distribution is mainly determined from the Earth's normal-mode frequencies and from the integral constraints of mean density and moment of inertia. We take the values of density in the Preliminary Reference Earth Model (PREM) (Dziewonski & Anderson 1981) and make comparisons over most of the depth range of the lower mantle. By sacrificing depth resolution in this way the density becomes accurately determined; averaged over a depth interval exceeding 1000 km, we expect the density to be known to better than 0.3–0.5 % (Gilbert *et al.* 1973). In fact, the analysis rests mainly on the density distribution between depths of 1000 and 2000 km because the shallower regions may be somewhat heterogeneous or anomalous, as may be deeper regions (especially the D″ layer), and the equations of state of minerals become

relatively uncertain at the pressures of depths exceeding 2000 km (see Dziewonski & Anderson 1981; Young & Lay 1987).

We begin by considering a model composition for the upper mantle, which is summarized in table 1 (all iron is listed as Fe^{2+}). This composition is derived mainly from analyses of mantle xenoliths, in addition to studies of ophiolite sequences and basalt petrogenesis (see, for example, Ringwood 1975; Yoder 1976; Green *et al.* 1979; Basaltic Volcanism Studies Project 1981). It corresponds to a garnet peridotite with roughly 55% olivine ($(Mg,Fe)_2SiO_4$) and 45% pyroxenes ($(Mg,Fe)SiO_3$ and $CaMgSi_2O_6$) and garnet (mainly $(Mg,Fe)_3Al_2Si_3O_{12}$), but because the olivine content is not critical for our analysis we allow the ratio of olivine to olivine and pyroxene to vary between $\frac{1}{2}$ and $\frac{2}{3}$. In contrast, the density is very sensitive to the iron content. In table 1, the ratio of MgO to MgO and FeO components is $x_{Mg} = 0.90$ (± 0.02). Although the majority of upper-mantle xenoliths yield $x_{Mg} = 0.90$–0.92 (Aoki 1984), we concentrate on the denser, iron-enriched limit ($x_{Mg} = 0.88$) for two reasons. First, the effect of partial melting is to deplete the iron out of the source region, so we are emphasizing the more fertile, unmelted compositions that represent the most primitive upper-mantle compositions that have been sampled. Second, the iron-rich composition comes closest to satisfying the observed density of the lower mantle. In fact, if the upper mantle actually has a composition with $x_{Mg} = 0.80$–0.86, our main conclusions either do not hold or cannot be proven with any certainty.

TABLE 1. MODELS OF UPPER-MANTLE COMPOSITION

oxide component	mass fraction (%)	element	atomic fraction (%)
SiO_2	45.0 ($\pm$1.4)	O	58.3
TiO_2	0.18 ($\pm$0.05)		
Al_2O_3	4.5 ($\pm$1.5)	Mg	20.1 ($\pm$1.0)
Cr_2O_3	0.4 ($\pm$0.1)	Si	15.8 ($\pm$0.5)
FeO	7.6 ($\pm$1.7)		
MnO	0.11 ($\pm$0.05)	Fe	2.2 ($\pm$0.5)
NiO	0.23 ($\pm$0.05)	Al	1.9 ($\pm$0.6)
MgO	38.4 ($\pm$2.0)	Ca	1.2 ($\pm$0.4)
CaO	3.3 ($\pm$1.0)		
Na_2O	0.4 ($\pm$0.2)	Na	0.27 ($\pm$0.14)
K_2O	0.01 ($\pm$0.1)	Cr	0.11 ($\pm$0.03)
total	100.1	Ni	0.06 ($\pm$0.01)
		Ti	0.05 ($\pm$0.01)
		Mn	0.03 ($\pm$0.01)
		K	0.004 ($\pm$0.04)

We note that the iron content is important mainly because of the large atomic mass of Fe: 55 against an average atomic mass of 21 for the composition in table 1. Thus, the density is controlled by the distribution of MgO, FeO and SiO_2 components, with the other constituents being present in small enough concentrations to be unimportant. The most abundant minor components, CaO and Al_2O_3, probably exist in a perovskite structured mineral at lower-mantle conditions, as do MgO, SiO_2 and (to a lesser degree) FeO. Whether the CaO and Al_2O_3 components enter into the Mg–Fe perovskite or form a separate perovskite (Liu & Bassett 1986), their contribution to the overall density appears to be negligible, according to currently available estimates (Jeanloz & Knittle 1986). Therefore, we evaluate the lower mantle composition in terms of the primary components MgO, FeO and SiO_2.

PHILOSOPHICAL TRANSACTIONS OF THE ROYAL SOCIETY A MATHEMATICAL, PHYSICAL & ENGINEERING SCIENCES

Mineralogy and temperature of the mantle

It is now well established that the olivine, pyroxene and garnet minerals existing in the upper mantle transform to denser phases when taken to the pressures of the transition zone and lower mantle (Jeanloz & Thompson 1983; Liu & Bassett 1986). The olivine is known to transform to the β-phase (spinelloid) and γ-spinel structures at the conditions of the transition zone (400–670 km depth), ultimately breaking down to a mixture of perovskite ($(Mg,Fe)SiO_3$) and magnesiowüstite ($(Mg,Fe)O$) at lower-mantle pressures. Over the same pressure interval, the pyroxenes and garnets react to form a silica-rich garnet (majorite) that trasforms to silicate perovskite at pressures existing near the top of the lower mantle. Thus, whether considered individually or as an assemblage, the dominant minerals of the upper mantle all form a silicate–perovskite assemblage at the conditions of the lower mantle.

Recent experiments demonstrate that $(Mg,Fe)SiO_3$ perovskite is stable throughout the entire pressure range of the lower mantle (Knittle & Jeanloz 1987). Therefore, we consider assemblages within the compositional range $2(Mg,Fe)SiO_3$ perovskite + $1(Mg,Fe)O$ magnesiowüstite (olivine:pyroxene ratio of 1) and $3(Mg,Fe)SiO_3$ perovskite + $2(Mg,Fe)O$ magnesiowüstite (olivine:pyroxene ratio of 2). The bulk composition is then completely specified by the olivine:pyroxene ratio and the x_{Mg} value, and the individual compositions of the perovskite and magnesiowüstite phases are obtained from the pressure-independent and temperature-independent partition coefficients of Bell *et al.* (1979) and Ito & Yamada (1982).

Because temperature and bulk composition together determine the density of a mineral assemblage, we consider the existing constraints on temperature in the mantle (figure 1). In the uppermost mantle, petrological studies offer the most direct estimates of temperature at depth (Jeanloz & Morris 1986). For example, the compositions of pyroxenes and garnets coexisting

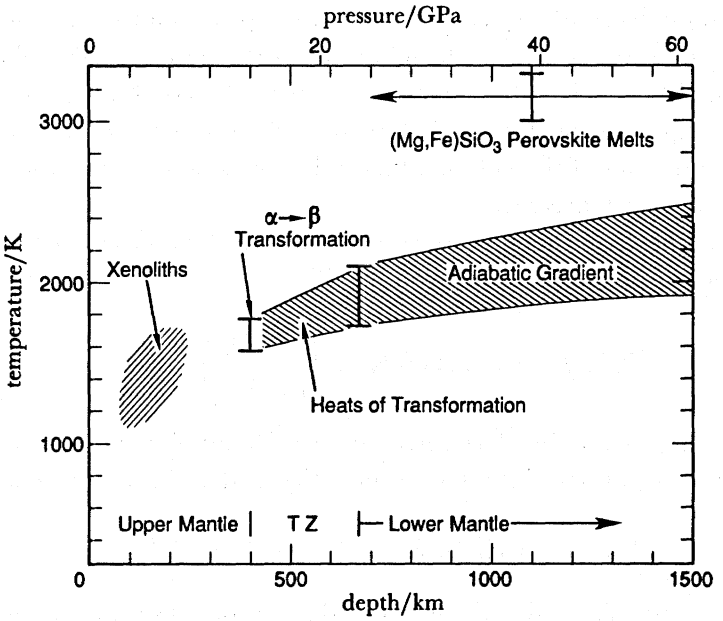

Figure 1. Constraints on temperature in the Earth's mantle shown as a function of depth (lower scale) and corresponding pressure (upper scale). Details are given in the text (see also Jeanloz & Morris 1986). TZ refers to the transition zone.

in xenoliths yield temperatures of 1600 (±200) K for a depth of 200 km. The seismologically observed discontinuities at 400 and 670 km depth also provide estimates of temperature if these discontinuities can be ascribed to equilibrium phase transitions. Both the pressure at 400 km depth and the changes in velocities across it are compatible with the 400 km discontinuity being caused by the transformation of olivine to β-phase (Weidner & Ito 1987). Therefore, considering experimental determinations of the transition pressure as a function of temperature yields an estimate near 1700 K for the top of the transition zone at 400 km depth (Jeanloz & Thompson 1983; Navrotsky & Akaogi 1984; Bina & Wood 1987). Adding the heats of transformation for the breakdown to a perovskite assemblage finally leads to a temperature at 670 km depth of 1950 K (Jeanloz & Thompson 1983; Navrotsky & Akaogi 1984).

This estimate is based on the assumption that there is convection through the transition zone: the adiabatic temperature change with depth is included, but no consideration is given to the possible contribution from a thermal boundary layer at the top of the lower mantle (see Jeanloz & Richter 1979). With this assumption, the extreme limits on the temperature at 670 km depth are 1720–2100 K. Continued extrapolation along an adiabatic gradient therefore provides a minimum estimate of temperatures within the convecting lower mantle. At 1500 km depth a temperature of 2200 K, with an absolute minimum of 1920 K, is obtained in this way (figure 1). For comparison, the melting experiments of Heinz & Jeanloz (1987) place an upper bound of 3000–3300 K for depths of 700–1500 km in the mantle.

Thermal equation of state

The effects of temperature and pressure on the volumes (hence the densities) of both perovskite and magnesiowüstite have been measured separately. To combine the data, interpolate to the simultaneous effects of pressure and temperature, and extrapolate the results to the conditions of the deep mantle it is necessary to use a physically based theory for the thermal equation of state. Recently we have derived an improved formalism that combines the eulerian finite-strain equation of state with the results of the perturbative anharmonic theory of lattice dynamics. Effectively, this gives us a way of combining room-temperature measurements of the equation of state with zero-pressure thermal-expansion data to obtain internally consistent estimates of the volume, thermal-expansion coefficient and bulk modulus as functions of pressure and temperature.

The pressure at volume V and temperature T is split into two terms, the 300 K isothermal pressure and the thermal pressure (P_{th}) at volume V

$$P(V, T) = P(V, 300\ \mathrm{K}) + \int_{300\ \mathrm{K}}^{T} \left(\frac{\partial P}{\partial \tau}\right)_V \mathrm{d}\tau. \tag{1}$$

The second term is then given by derivatives of the Helmholtz free energy, $(\partial P/\partial T)_V = -\partial^2 F/\partial V \partial T$, which is separated into harmonic (F_{H}) and anharmonic contributions (see Wallace 1972)

$$F(V, T) = F_{\mathrm{H}}(T, V) + A_0(V) + A_2(V)\, T^2. \tag{2}$$

For the present case, electronic, magnetic and disordering contributions to F are ignored, and the A_0 term is lost in the differentiation with respect to temperature. Thus, our analysis is limited to vibrational contributions to the thermal properties.

PHILOSOPHICAL TRANSACTIONS OF THE ROYAL SOCIETY A MATHEMATICAL, PHYSICAL & ENGINEERING SCIENCES

The philosophy behind this approach is to attempt only to fit data at temperatures of 300 K and above. Therefore, the dependency of F_H on the lattice vibrational spectrum is minimal and we consider only an average frequency, $\bar{\omega}$: more than a single characteristic frequency cannot be resolved in our analysis (see Jeanloz 1987). We identify $\bar{\omega}$ with the Einstein frequency (Einstein temperature $\theta_E = \hbar\bar{\omega}/k$), and set the corresponding Debye temperature to $\theta_D = \sqrt{\frac{5}{3}}\theta_E$ (Wallace 1972). With this correspondence between Einstein and Debye models we can verify that our data analysis is insensitive to the particular vibrational spectrum that is used, depending only on the characteristic frequency. We find this approximation to hold quite accurately (well within the quoted uncertainties) and can therefore set the thermal pressure to

$$P_{th}(T, V) = (\bar{\gamma}/V)\,[E_H(T, V) - E_H(300\text{ K}, V)] - \left(\frac{\partial A_2}{\partial V}\right)_T (T^2 - (300\text{ K})^2). \tag{3}$$

Both Einstein and Debye models are used for the harmonic internal energy, E_H, and the average Grüneisen parameter is defined by

$$\bar{\gamma} = (-\partial \ln \bar{\omega}/\partial \ln V)_T. \tag{4}$$

The advantage to this approach is that it combines two, physically based formulations that are empirically known to successfully describe existing measurements. These are the Eulerian finite-strain equation of state (see, for example, Birch 1952, 1978; Jeanloz & Knittle 1986; Jeanloz & Grover 1988; Jeanloz 1988, 1989) and the anharmonic description of thermal properties (Leibfried & Ludwig 1961; Zharkov & Kalinin 1971; Wallace 1972). The resulting expression for thermal expansion involves a more realistic equation of state (strain energy–volume relation) and, because the reference temperature is 300 K rather than 0 K, less sensitivity to the detailed vibrational spectrum than previous formulations, such as Suzuki's (1975). This is desirable for geophysical applications to high temperatures and pressures, but would not be so for low-temperature applications.

We fit (1) and (3) by first deriving the values of bulk modulus (K_0) and its pressure derivative (K_0') that reproduce the isothermal equation of state according to Birch's finite-strain formalism (truncated to third order in strain; see Birch 1978, for example). Then, the zero-pressure thermal expansion data are fitted to (1) by setting $-P(V, 300\text{ K}) = P_{th}(T, V)$ (i.e. $P(V, T) = 0$) to yield values of $\theta_{0D}, \bar{\gamma}_0, q$ and $q_2 A_{20}$. The Grüneisen parameter describes the volume dependence of the characteristic temperature according to (4), subscripts zero indicate ambient conditions ($P = 0$, $T = 300$ K), and

$$q = \mathrm{d} \ln \bar{\gamma}/\mathrm{d} \ln V, \tag{5}$$

$$q_2 = \mathrm{d} \ln A_2/\mathrm{d} \ln V \tag{6}$$

are assumed constant and of order unity. Note that $\bar{\omega}$, θ_D, $\bar{\gamma}$ and A_2 depend directly only on volume in this approach; indirectly they depend on temperature through the thermal expansion, but this is only significant for $\bar{\omega}$ or θ_D. The entire thermal equation of state, $P(V, T)$, is then given by the V_0, K_0, K_0', θ_{0D}, $\bar{\gamma}_0$, q, and the product $q_2 A_{20}$. These parameters are obtained by nonlinear least-squares fitting, in which equation-of-state and thermal-expansion measurements are weighted by the reciprocal of their pressure-dependent and temperature-dependent variances.

The resulting values for silicate perovskite and magnesiowüstite are listed in table 2. Here, $x_{Fe}\,(=1-x_{Mg})$ is the amount of iron component, but it should be noted that most of the measurements on which the values are based were obtained from Mg-rich samples. Primarily, we used the $T = 300$ K static-compression measurements of Knittle & Jeanloz (1987) on $Mg_{0.88}Fe_{0.12}SiO_3$ perovskite, along with Jackson & Niesler's (1982) ultrasonic data on MgO to 3.0 GPa (from which a 300 K compression curve is derived). The $P = 0$ thermal expansion measurements are those of Knittle *et al.* (1986) on perovskite of the same composition and of Suzuki (1975) on MgO. Uncertainties in the measurements have been propagated to the values given in table 2, and the effects of varying composition (Mg/Fe ratio) on the properties are discussed by Jackson *et al.* (1978), Jeanloz & Thompson (1983) and Williams *et al.* (1988).

Figures 2 and 3 summarize the data for perovskite and magnesiowüstite, along with the pressure–volume relations derived from the parameters in table 2. Because the pressure depends almost entirely on volume, it is evident that the 300 K isotherm is of primary importance for constraining the thermal equation of state. In comparison, the harmonic and

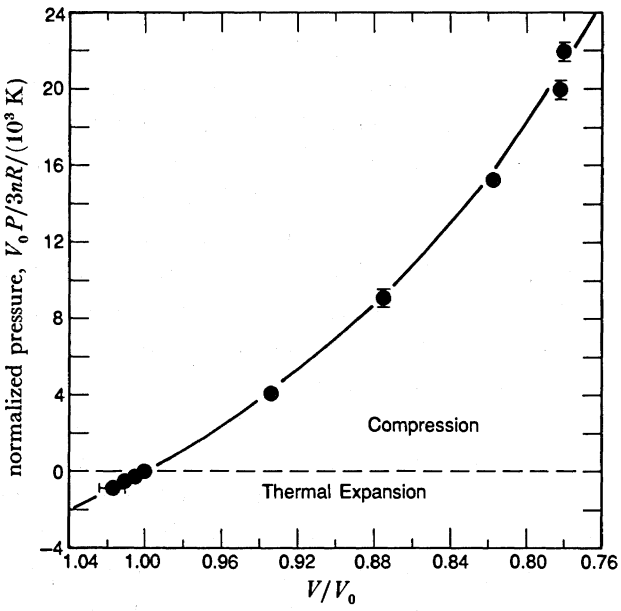

FIGURE 2. Thermal equation of state of $(Mg,Fe)SiO_3$ perovskite: summary of data (symbols with error bars) and model (curve) based on the parameters given in table 2 (see text).

TABLE 2. PHYSICAL PROPERTIES AT $P = 0$, $T = 300$ K

	perovskite $(Mg,Fe)SiO_3$	magnesiowüstite $(Mg,Fe)O$
volume, $V_0/(cm^3\ mol^{-1})$	$24.46\ (\pm0.04)+1.03\ (\pm0.28)x_{Fe}$	$11.25\ (\pm0.001)+1.00\ (\pm0.02)x_{Fe}$
atoms in formula, n	5	2
bulk modulus, K_0/GPa	266 (±6)	160.1 (±0.3)
pressure derivative, K_0'	3.9 (±0.4)	4.1 (±0.1)
Debye temperature, θ_0/K	725 (±25)	782 (±20)
Grüneisen parameter, γ_0	1.70 (±0.05)	1.66 (±0.02)
volume dependence, q	1 (±1)	1 (±1)
anharmonic term, $(q_2 A_{20}/3nR)/K^{-1}$	$-1.2\ (\pm0.9)\times10^{-4}$	$0.92\ (\pm0.08)\times10^{-4}$

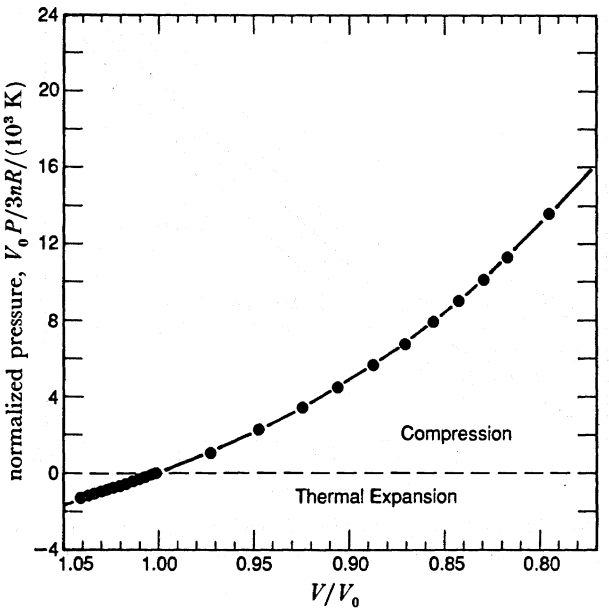

FIGURE 3. Thermal equation of state of MgO periclase: summary of data (symbols with error bars) and model (curve) based on the parameters given in table 2.

anharmonic thermal corrections are of secondary importance. We emphasize this point because it shows that to first order the density of the lower mantle is being compared with a measurement, not an extrapolation, of a mineral assemblage density at lower-mantle conditions. The importance of ultra-high-pressure measurements in this regard is also discussed by Bell *et al.* (1987).

RESULTS AND DISCUSSION

The thermal equation of state model for Mg–Fe silicate perovskite is illustrated in figure 4. Here the temperature is held constant at 2000 K, a plausible value for the deep mantle, and the effect of varying x_{Mg} is shown; the raw data making up the 300 K isotherm are also included for reference in this and the following two figures. Varying the iron content affects the density in two ways: primarily through the molar mass and secondarily through the molar volume (table 2). These effects are opposite in sign, but the first far outweighs the second.

The basic conclusion of our study is already evident in figure 4, even though this refers only to a pure pyroxene composition. For a typical upper-mantle value of $x_{Mg} = 0.90$, the density of perovskite is significantly less than that observed for the lower mantle. At 2000 K the discrepancy is 2 (± 1) %. As we point out below, this is a minimum value for the intrinsic density difference between the upper and lower mantle if these regions indeed differ in bulk composition. By intrinsic we mean a comparison at a given pressure and temperature. Although the effects on the density difference of varying temperature and silica content (ratio of olivine to pyroxene components) also need to be considered, these do not alter our initial conclusion.

Figure 5 summarizes the effect of temperature on the pressure–density relations of the four perovskite compositions that were considered in figure 4. It is clear that for a minimum estimated temperature in the deep mantle (*ca.* 1000–2000 km depth) of about 1900–2200 K,

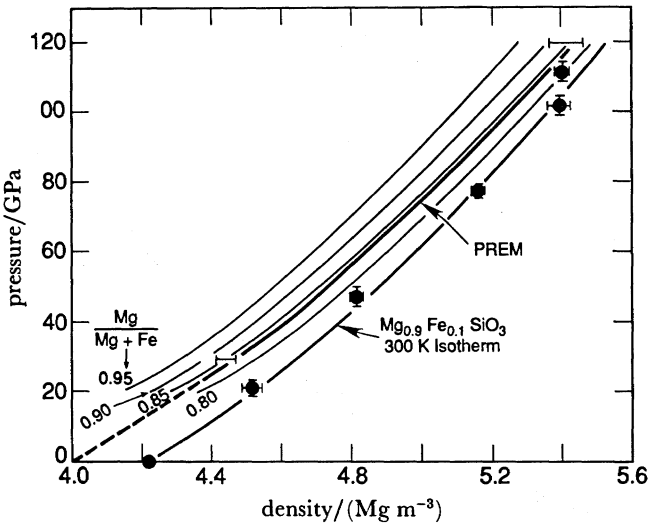

FIGURE 4. Isotherms (2000 K) for $(Mg,Fe)SiO_3$ perovskite of varying x_{Mg} content according to the present thermal equation of state model. Representative uncertainties are shown at $P = 30$ GPa and 120 GPa along the $x_{Mg} = 0.85$ isotherm.

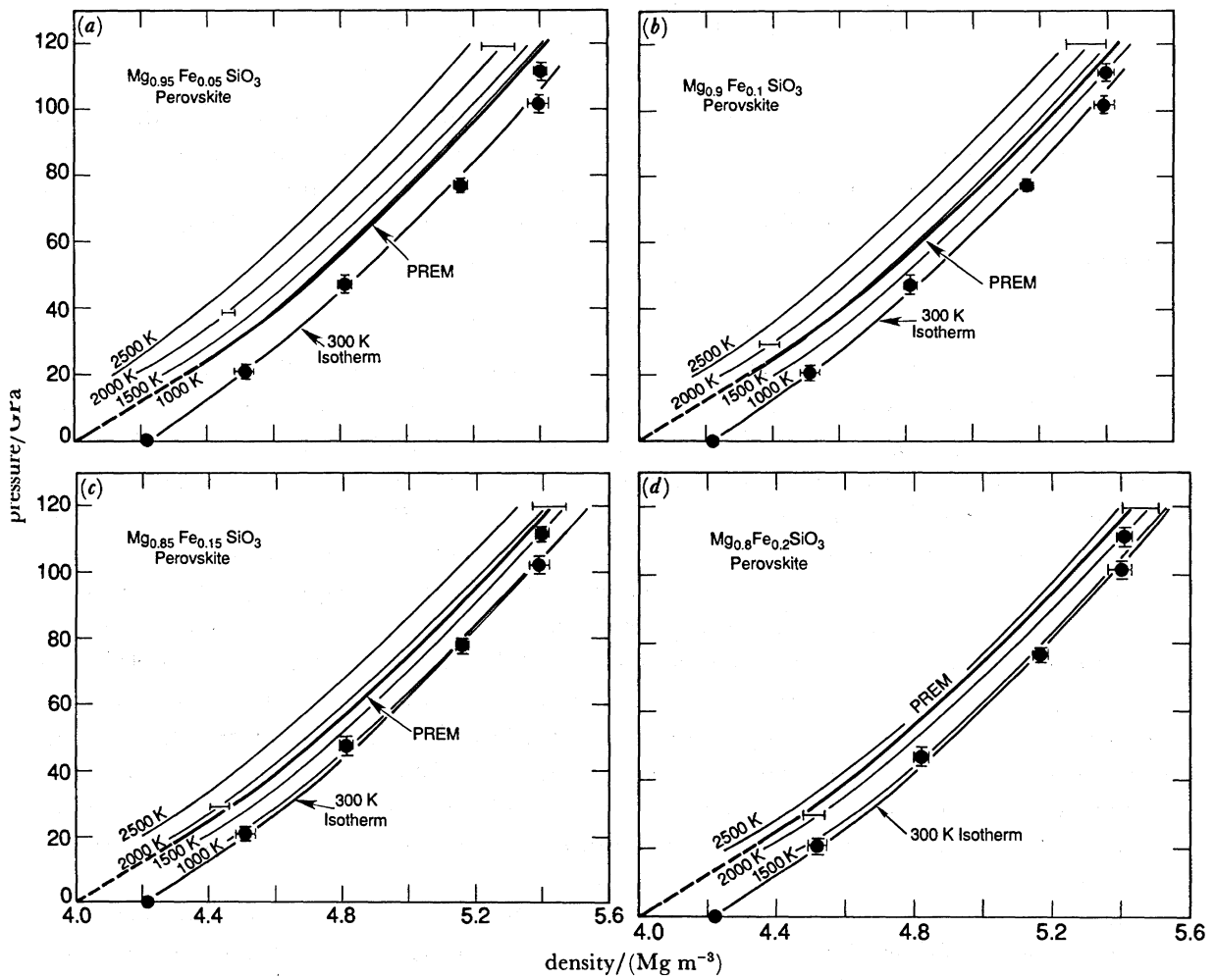

FIGURE 5. Isotherms for $(Mg,Fe)SiO_3$ perovskite according to the present thermal equation of state model, for compositions of $x_{Mg} = 0.95$ (*a*), 0.90 (*b*), 0.85 (*c*), and 0.80 (*d*). Representative uncertainties are shown at $P = 30$–40 GPa and 120 GPa along the $T = 2000$ K isotherm.

the largest acceptable value of x_{Mg} is in the range of 0.80–0.85. That is, considering only the silicate perovskite constituent and assuming no thermal boundary later at the 670 km discontinuity, a best estimate of $T = 2200$ K requires the ratio of MgO to MgO + FeO components to equal 0.79 (± 0.01). Although the lower-mantle geotherm is expected to be adiabatic, because this region is thought to be convecting vigorously, we only show isotherms for the pressure-density relations (see, for example, Jeanloz & Morris 1986). We do this both for simplicity and because the difference between an isotherm and an adiabat is probably less than our resolution. Nevertheless, there is a suggestion in figure 5 that higher temperature (hence greater iron content) leads to density profiles that are more compatible with the lower mantle being adiabatic. For example, the pressure–density relations make PREM appear to follow a sub-isothermal (let alone subadiabatic) trend in figure 5*a*, whereas it appears more nearly adiabatic in the comparisons shown in figure 5*c*, *d* (within the uncertainties).

The addition of magnesiowüstite (effectively, olivine component) hardly changes these calculations (figure 6). A limiting upper-mantle composition of $x_{Mg} = 0.88$ requires lower-mantle temperatures of about 1400 K, whereas a minimum estimate of 1900–2000 K for the lower mantle implies a composition of $x_{Mg} = 0.84$. These results are shown in figure 7, which summarizes from figures 5 and 6 the combinations of composition and temperature that are required to match the observed density of the lower mantle. Thus, a conventional estimate of upper-mantle composition ($x_{Mg} = 0.90$) would necessitate a temperature of 1200 (± 300) K in the lower mantle were the composition held constant.

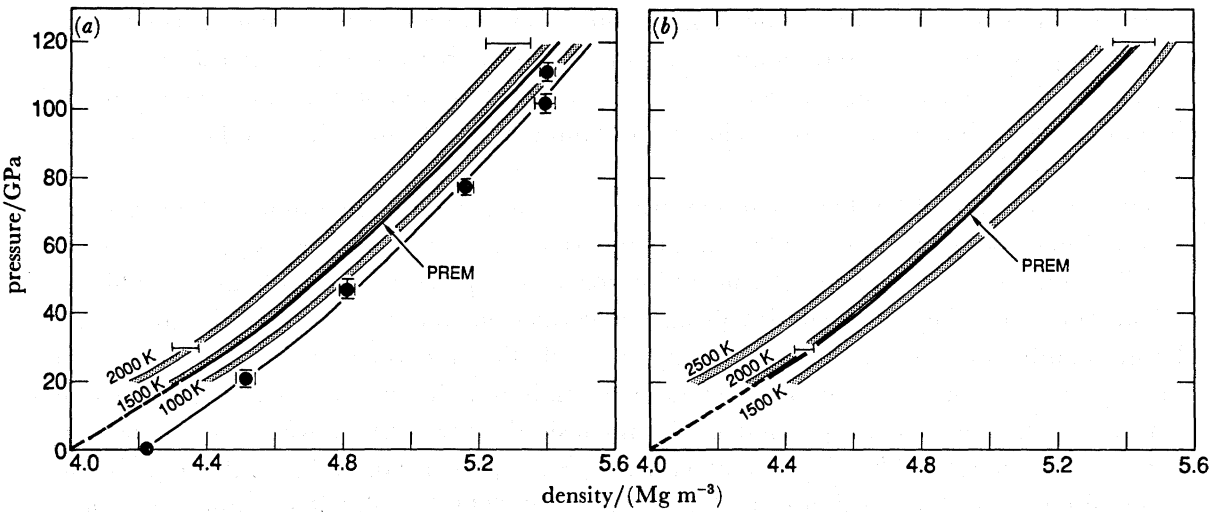

FIGURE 6. Isotherms for combinations of (Mg,Fe)SiO_3 perovskite and (Mg,Fe)O magnesiowüstite with total x_{Mg} of the assemblage being 0.88 (*a*) and 0.84 (*b*). Partition coefficients for Fe and Mg distributed between perovskite and magnesiowüstite are from Bell *et al.* (1979) and Ito & Yamada (1982). The width of shading for each isotherm reflects variations in composition between 2 perovskite + 1 magnesiowüstite and 3 perovskite + 2 magnesiowüstite.

Our attempt has been to be conservative in this analysis, tending to overstate the estimated uncertainties involved. Yet it is clear that if the upper mantle is more magnesium-rich than $x_{Mg} = 0.88$ and if the bulk of the lower mantle is at a temperature above 1900 K, then the lower mantle is intrinsically denser than would be expected for an upper-mantle composition: i.e. a model of uniform mantle composition. Unless the mineralogical constitution of the lower

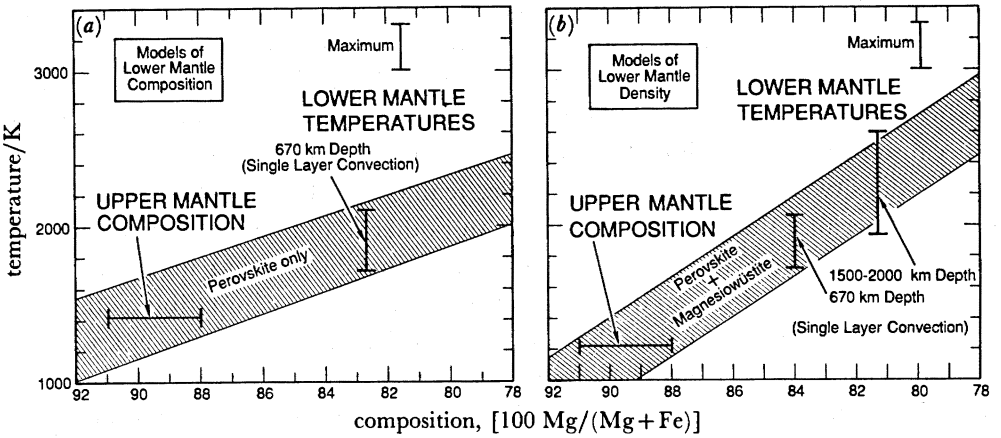

FIGURE 7. Tradeoff between composition (x_{Mg}) and temperature required to satisfy the observed density of the lower mantle. Assemblages of perovskite alone (*a*) and perovskite + magnesiowüstite in ratios between 2:1 and 3:2 (*b*) are shown.

mantle differs significantly from an assemblage dominated by $(Mg,Fe)SiO_3$ perovskite, as outlined above, the existing measurements of perovskite density at high pressures and temperatures lead inevitably to this conclusion. Specifically, one needs to invoke the presence in the lower mantle of an unknown, denser phase, that is either much denser than the perovskite or very abundant, to avoid this conclusion. So far, there is no evidence for the existence of such a mineral phase despite numerous synthesis experiments carried out at the appropriate pressures and temperatures (Yagi *et al.* 1979; Liu & Bassett 1986; Knittle & Jeanloz 1987). Therefore, we conclude that a model of uniform mantle composition is incompatible with the current seismological and mineralogical constraints on the density of the lower mantle.

Despite the strength of this conclusion, we cannot derive a unique estimate of lower mantle composition from our analysis. There are two reasons for this. First, our results are insensitive to silica content, or the ratio of olivine and pyroxene components (figures 6 and 7). This is an advantage in making our analysis robust, but it rules out the possibility of our constraining lower mantle composition unambiguously. Second, the tradeoff between temperature and density is such that we can only estimate a minimum density difference (compositional contrast) with any reliability. That is, the intrinsic density of the lower mantle, compared between 1000 and 2000 km depth, is at least 2.6 (± 1) % greater than that of the upper mantle composition according to figure 6*a* ($x_{Mg} \geqslant 0.88$, $T \geqslant 2000$ K). But if the upper and lower mantle differ in composition, they cannot intermix significantly over geological timescales, and they must therefore be separately convecting systems. In this instance of layered mantle convection, the temperature of the lower mantle would be expected to be at least 500 K higher than in the case of single-layer convection because of the presence of an extra thermal boundary layer near 700 km depth (Jeanloz & Richter 1979). The result is to increase the required contrast in intrinsic density between the upper and lower mantle to about 5 (± 2) %. In principle, the upper limit of 3000–3300 K for the temperature of the lower mantle (figure 1) bounds this value from above. In practice, however, the extrapolation of the equations of state becomes rapidly less certain with increasing temperature because the anharmonic contributions are not well determined at high pressures and temperatures. Therefore, it is difficult to

PHILOSOPHICAL TRANSACTIONS OF THE ROYAL SOCIETY A MATHEMATICAL, PHYSICAL & ENGINEERING SCIENCES

uniquely identify the intrinsic density difference between the upper and lower mantle, and the compositional contrast is even less uniquely determined.

The arguments presented here are simplistic in that they ignore the lateral variations in composition, mineralogical constitution and temperature that must inevitably exist in the lower mantle (e.g. simply as a consequence of convective heat transfer). Therefore, we do not claim that the mantle must be rigidly layered. Locally dense or buoyant material can penetrate through the 670 km discontinuity if either the composition or temperature varies sufficiently to counteract the *ca.* 3–5 % intrinsic density contrast that we have estimated for the lower and upper mantle. In this sense the layering can be leaky, with the only limitation being that there has been insufficient mass transfer over geological history to completely homogenize the mantle. Because the original difference that may have existed between upper and lower mantle compositions is unknown, as is its evolution in time, there is no reason to rule out a finite (but incomplete) amount of intermixing between these regions.

Were there to be intermixing, the associated heat transfer would diminish the thermal boundary layer between the upper and lower mantle. Indeed, laboratory experiments suggest that partial, local intermixing may be inevitable at the interface between separately convecting fluids (H. Nataf, personal communication 1983; Olson 1984; Silver *et al.* 1988). In addition, there is some evidence that the viscosity of the lower mantle may be 1–2 orders of magnitude larger than that of the upper mantle (Hager 1984). Both the intermixing and the viscosity change are likely to smear out or at least obscure the presence of a thermal boundary layer. It is because of these complications that we have confined our analysis to a simple comparison of observed and modelled densities over the approximate depth range of 1000 to 2000 km, and assuming values of $x_{\mathrm{Mg}} = 0.88$ for the upper mantle composition and 1900–2200 K for the temperature through most of the lower mantle.

Conclusions

Synthesis experiments at elevated pressures and temperatures indicate that the lower mantle consists almost entirely of $(\mathrm{Mg,Fe})\mathrm{SiO_3}$ perovskite coexisting with (Mg,Fe)O magnesiowüstite. Thermal equations of state for these two minerals, either separately or in combination, are well constrained by existing measurements; in particular, the effect of pressure on density is well known up to the 100 GPa range. Consequently, the density distribution throughout the lower mantle can be modelled with little uncertainty. We find that if (i) the upper mantle is characterized by an iron/magnesium content of $x_{\mathrm{Mg}} = 0.90$ (± 0.02), and (ii) the lower mantle is at a temperature of 2200 (± 300) K or above, then the observed density distribution through the lower mantle cannot be satisfied with an upper mantle composition (barring the presence of an unknown, sufficiently dense and abundant new phase). Therefore, the upper and lower mantle appear to differ in bulk composition. The intrinsic density difference between these regions is estimated to be about 3–5 %, with a minimum value of 2.6 (± 1) %, and this is sufficient to keep the mantle dynamically stratified (see Richter & McKenzie 1981; Olson 1984). These results suggest that the average temperature in the deep mantle exceeds 2200 K and that samples of the uppermost mantle are not representative of the bulk of the mantle.

We have benefited from discussions with T. G. Masters, D. L. Anderson, T. J. Ahrens and B. H. Hager, and from the comments of F. R. Boyd and D. Price. This work was funded by the

PHILOSOPHICAL TRANSACTIONS OF THE ROYAL SOCIETY A MATHEMATICAL, PHYSICAL & ENGINEERING SCIENCES

National Science Foundation. R.J. is grateful for the generous support provided by the Fairchild Scholar programme (California Institute of Technology) during the preparation of this manuscript.

References

Aoki, K. 1984 In *Materials science of the Earth's interior* (ed. I. Sunagawa), pp. 415–444. Tokyo: Terra Scientific.

Basaltic Volcanism Study Project 1981 *Basaltic volcanism on the terrestrial planets.* (1286 pages.) New York: Pergamon.

Bell, P. M., Mao, H. K. & Xu, J. A. 1987 In *High pressure research in mineral physics* (ed. M. Manghnani and Y. Syono), pp. 447–454. Washington: American Geophysical Union.

Bell, P. M., Yagi, T. & Mao, H. R. 1979 Iron-magnesium distribution coefficients between spinel [$(Mg,Fe)_2SiO_4$], magnesiowüstite [(Mg,Fe)O] and perovskite [$(Mg,Fe)SiO_3$]. *Carnegie Inst. Wash. Yb.* **78**, 618–621.

Bina, C. R. & Wood, B. J. 1987 The olivine-spinel transition: experimental and thermodynamic constraints and implications for the nature of the 400 km seismic discontinuity. *J. geophys. Res.* **92**, 4853–4866.

Birch, F. 1952 Elasticity and constitution of the Earth's interior. *J. geophys. Res.* **57**, 272–286.

Birch, F. 1978 Finite strain isotherm and velocities for single-crystal and polycrystalline NaCl at high pressures and 300 °K. *J. geophys. Res.* **83**, 1257–1268.

Dziewonski, A. M. & Anderson, D. L. 1981 Preliminary reference Earth model. *Physics Earth planet. Inter.* **25**, 297–356.

Gilbert, F., Dziewonski, A. & Brune, J. 1973 An informative solution to a seismological inverse problem. *Proc. natn. Acad. Sci. U.S.A.* **70**, 1410–1413.

Green, D. H., Hibberson, W. O. & Jacques, A. L. 1979 In *The Earth: its origin, structure and evolution* (ed. M. W. McElhinny), pp. 265–299. New York: Academic Press.

Hager, B. H. 1984 Subducted slabs and the geoid: constraints on mantle rheology and flow. *J. geophys. Res.* **89**, 6003–6015.

Heinz, D. L. & Jeanloz, R. 1987 Measurement of the melting curve of $(Mg,Fe)SiO_3$ at lower mantle conditions and its geophysical implications. *J. geophys. Res.* **92**, 11437–11444.

Ito, E. & Yamada, H. 1982 Stability relations of silicate spinels, ilmenites and perovskites. In *High pressure research in geophysics* (ed. S. Akimoto & M. H. Manghnani), pp. 405–419. Tokyo: Center for Academic Publishing.

Jackson, I. & Niesler, H. 1982 The elasticity of periclase to 3 GPa and some geophysical implications. In *High pressure research in geophysics* (ed. S. Akimoto & M. H. Manghnani), pp. 93–113. Tokyo: Center for Academic Publishing.

Jackson, I., Liebermann, R. C. & Ringwood, A. E. 1978 The elastic properties of $(Mg_xFe_{1-x})O$ solid solutions. *Phys. Chem. Miner.* **3**, 11–31.

Jeanloz, R. 1987 Coexistence curves and equilibrium boundaries for high-pressure phase transformations. *J. geophys. Res.* **92**, 10352–10362.

Jeanloz, R. 1988 Universal equation of state. *Phys. Rev.* B. **38**, 805–807.

Jeanloz, R. 1989 Shock-wave equation of state and finite-strain theory. *J. geophys. Res.* (In the press.)

Jeanloz, R. & Grover, R. 1988 Birch-Murnaghan and U_s-up equations of state. In *Shock Waves in Condensed Matter* (ed. E. C. Schmidt & N. C. Holmes), pp. 69–72. New York: North-Holland.

Jeanloz, R. & Knittle, E. 1986 Reduction of mantle and core properties to a standard state by adiabatic decompression. *Adv. Phys. Geochem.* **6**, 275–309.

Jeanloz, R. & Morris, S. 1986 Temperature distribution in the crust and mantle. *A. Rev. Earth planet. Sci.* **14**., 377–415.

Jeanloz, R. & Richter, F. M. 1979 Convection, composition and the thermal state of the lower mantle. *J. geophys. Res.* **84**, 5497–5504.

Jeanloz, R. & Thompson, A. B. 1983 Phase transitions and mantle discontinuities. *Rev. Geophys. space Phys.* **21**, 51–74.

Knittle, E. & Jeanloz, R. 1987 Synthesis and equation of state of $(Mg,Fe)SiO_3$ perovskite to over 100 GPa. *Science, Wash.* **235**, 668–670.

Knittle, E., Jeanloz, R. & Smith, G. 1986 The thermal expansion of silicate perovskite and stratification of the Earth's mantle. *Nature, Lond.* **319**, 214–216.

Leibfried, G. & Ludwig, W. 1961 Theory of anharmonic effects in crystals. *Solid St. Phys.* **12**, 275–444.

Liu, L. & Bassett, W. A. 1986 *Elements, oxides and silicates.* (250 pages.) New York: Oxford University Press.

Navrotsky, A. & Akaogi, M. 1984 α-β-γ phase relations in Fe_2SiO_4–Mg_2SiO_4 and Ca_2SiO_4–Mg_2SiO_4: calculation from thermochemical data and geophysical applications. *J. geophys. Res.* **89**, 10135–10 140.

Olson, P. 1984 An experimental approach to thermal convection in a two-layered mantle. *J. geophys. Res.* **89**, 11293–11301.

Richter, F. M. & McKenzie, D. P. 1981 On some consequences and possible causes of layered mantle convection. *J. geophys. Res.* **86**, 6133–6142.

PHILOSOPHICAL TRANSACTIONS OF THE ROYAL SOCIETY A MATHEMATICAL, PHYSICAL & ENGINEERING SCIENCES

Ringwood, A. E. 1975 *Composition and petrology of the Earth's mantle*. (618 pages.) New York: McGraw-Hill.
Silver, P. G., Carlson, R. W. & Olson, P. 1988 Deep slabs, geochemical heterogeneity and the large-scale structure of mantle convection: investigation of an enduring paradox. *A. Rev. Earth planet. Sci.* **16**, 477–541.
Suzuki, I. 1975 Thermal expansion of periclase and olivine, and their anharmonic properties. *J. Phys. Earth* **23**, 145–159.
Wallace, D. C. 1972 *Thermodynamics of crystals*. (484 pages.) New York: Wiley.
Weidner, D. J. & Ito, E. 1987 In *High pressure research in mineral physics* (ed. M. Manghnani & Y. Syono), pp. 439–446. Washington: American Geophysical Union.
Williams, Q., Knittle, E. & Jeanloz, R. 1988 Geophysical and crystal chemical significance of $(Mg,Fe)SiO_3$ perovskite. *Mineral Physics Monograph* no. 3. Washington D.C.: Am. Geophys. Union. (In the press.)
Yagi, T., Bell, P. M. & Mao, H. K. 1979 Phase relations in the system $MgO–FeO–SiO_2$ between 150 and 700 kbar at 1000 °C. *Carnegie Inst. Wash. Yb.* **78**, 614–618.
Yoder, H. S. Jr 1976 *Generation of basaltic magmas*. (265 pages.) Washington: National Academy of Sciences.
Young, C. J. & Lay, T. 1987 The core-mantle boundary. *A. Rev. Earth planet. Sci.* **15**, 35–46.
Zharkov, V. N. & Kalinin, V. A. 1971 *Equation of state for solids at high pressure and temperatures*. New York: Consultants Bureau.

PHILOSOPHICAL TRANSACTIONS OF THE ROYAL SOCIETY A MATHEMATICAL, PHYSICAL & ENGINEERING SCIENCES